Bicollinear Antiferromagnetic Order, Monoclinic Distortion, and Reversed Resistivity Anisotropy in FeTe as a Result of Spin-Lattice Coupling

Christopher B. Bishop, Adriana Moreo, and Elbio Dagotto
Department of Physics and Astronomy, University of Tennessee, Knoxville, Tennessee 37966, USA
and Materials Science and Technology Division, Oak Ridge National Laboratory, Oak Ridge, Tennessee 37831, USA
(Received 2 June 2016; published 8 September 2016)

The bicollinear antiferromagnetic order experimentally observed in FeTe is shown to be stabilized by the coupling $\tilde{g}_{12}$ between monoclinic lattice distortions and the spin-nematic order parameter with B_{2g} symmetry, within a three-orbital spin-fermion model studied with Monte Carlo techniques. A finite but small value of $\tilde{g}_{12}$ is required, with a concomitant lattice distortion compatible with experiments, and a tetragonal-monoclinic transition strongly first order. Remarkably, the bicollinear state found here displays a planar resistivity with the "reversed" puzzling anisotropy discovered in transport experiments. Orthorhombic distortions are also incorporated, and phase diagrams interpolating between pnictides and chalcogenides are presented. We conclude that the spin-lattice coupling we introduce is sufficient to explain the challenging properties of FeTe.

DOI: 10.1103/PhysRevLett.117.117201

Introduction.—The chalcogenide FeTe is an unusual member of the iron-based superconductor family [1–4]. Angle-resolved photoemission (ARPES) [5] for FeTe revealed substantial mass renormalizations indicative of electrons that are more strongly interacting than in pnictides (see also Ref. [6]). The absence of Fermi surface (FS) nesting instabilities was also established [7,8]. Moreover, using single-crystal neutron diffraction, "bicollinear" magnetism was reported in FeTe [9]. This exotic antiferromagnetic (AFM) state is known as the E phase in manganites [10]. Phenomenological approaches rationalize the bicollinear state based on Heisenberg J_1-J_2-J_3 models [11] if the furthest distance coupling J_3 is assumed to be robust. Effective spin models [11,12] are certainly valid descriptions after the lattice distortion occurs, but they do not illuminate the fundamental reasons for the bicollinear state stability [13–15].

Upon cooling, experimentally the bicollinear state is reached via a robust first-order phase transition [9,16,17], with a concomitant tetragonal ($\mathcal{T}_{\rm etra}$) to monoclinic ($\mathcal{M}_{\rm ono}$) lattice distortion. The reported distortions in $Fe_{1.076}Te$ and $Fe_{1.068}Te$ are $\delta_M = |a_M - b_M|/(a_M + b_M) \sim 0.007$ [9] (a_M and b_M are the low-temperature lattice parameters in the $\mathcal{M}_{\rm ono}$ notation). This distortion is comparable to the orthorhombic ($\mathcal{O}_{\rm rth}$) lattice distortion in $BaFe_2As_2$ [18] $\delta_O = |a_O - b_O|/(a_O + b_O) \sim 0.004$ (now with a_O and b_O the low-temperature lattice parameters in the $\mathcal{O}_{\rm rth}$ notation). Since the lattice is considered a "passenger" in the pnictides, it may be suspected that it also plays a secondary role for chalcogenides [19].

Contrary to this reasoning, here we argue that the lattice may play a more fundamental role in FeTe than previously anticipated. Specifically, we construct a spin-fermion (SF) model where lattice and spins are coupled in a manner that includes the $\mathcal{M}_{\rm ono}$ distortion of FeTe. Using Monte Carlo techniques, we found a strong first-order $\mathcal{T}_{\rm etra}$ to $\mathcal{M}_{\rm ono}$ lattice transition, as in experiments [9]. Moreover, the bicollinear magnetic order spontaneously arises at the same critical temperature. All this is achieved with a (dimensionless) spin-lattice coupling $\tilde{g}_{12} \gtrsim 0.10$–$0.25$ that is not strong. Surprisingly, we also find the same puzzling *reversed* anisotropy in the low-temperature resistivity recently reported [20,21], with the AFM direction more resistive than the ferromagnetic (FM), contrary to results in pnictides.

We also include the spin-lattice coupling $\tilde{g}_{66}$ that favors orthorhombicity, although in this case the crystal's geometry—with nearest-neighbor (NN) and next-NN (NNN) hoppings of similar strength and associated FS nesting—already favors the concomitant $(\pi, 0)$ collinear magnetism even without the lattice. Our analysis interpolates between (collinear) pnictides and (bicollinear) chalcogenides using the *same* hopping amplitudes because band structure calculations give similar results for both [22]. In fact, the high-temperature regime displays a FS with the canonical hole-electron pockets, naively suggesting that only $\mathcal{O}_{\rm rth}$ and $(\pi, 0)$ spin order could be stabilized. However, our calculations show that strong first-order transitions can induce a low-temperature state with no precursors at high temperatures.

The presence of both itinerant and localized characteristics in neutron experiments for $Fe_{1.1}Te$ [23] suggests that the SF model provides a proper framework. While we cannot fully incorporate the electronic interactions, the Hund coupling of the SF model mimics a Hubbard U by reducing double occupancy at each orbital [8]. In these respects, our study has the same accuracy as in the successful description of manganites [10,24].

Model.—The SF Hamiltonian used here is based on the original purely electronic model [25,26], supplemented by couplings to the lattice degrees of freedom [27,28]

$$H_{\mathrm{SF}} = H_{\mathrm{Hopp}} + H_{\mathrm{Hund}} + H_{\mathrm{Heis}} + H_{\mathrm{Stiff}} + H_{\mathrm{SLO}} + H_{\mathrm{SLM}}. \tag{1}$$

H_{Hopp} is the three-orbital (d_{xz}, d_{yz}, d_{xy}) tight-binding Fe-Fe hopping of electrons, with hopping amplitudes selected to reproduce ARPES data [see Eqs. (1)–(3) and Table 1 of Ref. [29]]. The undoped-limit average electronic density per iron and per orbital is $n = 4/3$ [29], and a chemical potential in H_{Hopp} [28] controls its value. The Hund interaction is $H_{\mathrm{Hund}} = -J_H \sum_{\mathbf{i},\alpha} \mathbf{S_i} \cdot \mathbf{s}_{\mathbf{i},\alpha}$, where $\mathbf{S_i}$ are localized spins at site $\mathbf{i}$ and $\mathbf{s}_{\mathbf{i},\alpha}$ are itinerant spins corresponding to orbital α at the same site [30]. Electrons in the nonitinerant orbitals $d_{x^2-y^2}$ and $d_{3z^2-r^2}$ are assumed to have hopping amplitudes smaller than for the itinerants, thus effectively increasing their Hubbard U to bandwidth W ratio. For this reason, a strong coupling expansion generates H_{Heis} that contains the NN and NNN Heisenberg interactions among those localized spins, with respective couplings J_{NN} and J_{NNN} and ratio $J_{\mathrm{NNN}}/J_{\mathrm{NN}} = 2/3$ [31]. The NN and NNN Heisenberg couplings are comparable because Fe-Fe hopping occurs via Te atoms at the center of Fe plaquettes [32]. However, we will show that J_{NN} and J_{NNN} are not crucial for our main conclusions. H_{Stiff} is the lattice stiffness (Lennard-Jones potential) to speed up convergence [27,28].

Previous SF model investigations addressed the $\mathcal{T}_{\mathrm{etra}}$-$\mathcal{O}_{\mathrm{rth}}$ transition as in $SrFe_2As_2$ [27]. The coupling of the spins with the $\mathcal{O}_{\mathrm{rth}}$ lattice distortion [27] is given by $H_{\mathrm{SLO}} = -g_{66} \sum_{\mathbf{i}} \Psi_{\mathbf{i}}^{NN} \epsilon_{66}(\mathbf{i})$ [33,34], where g_{66} is the canonical $\mathcal{O}_{\mathrm{rth}}$ spin-lattice coupling [35] and the spin NN nematic order parameter is

$$\Psi_{\mathbf{i}}^{NN} = \frac{1}{2} \mathbf{S_i} \cdot (\mathbf{S_{i+y}} + \mathbf{S_{i-y}} - \mathbf{S_{i+x}} - \mathbf{S_{i-x}}), \tag{2}$$

where $\mathbf{x}$ and $\mathbf{y}$ are unit vectors along the x and y axes, respectively. $\Psi_{\mathbf{i}}^{\mathrm{NN}}$ is 2 in the perfect $(\pi, 0)$ state shown in Fig. 1(a). $\epsilon_{66}(\mathbf{i})$ is the lattice $\mathcal{O}_{\mathrm{rth}}$ strain defined in terms of the positions of the As, Se, or Te atoms with respect to their neighboring Fe. Its precise definition is [27]

$$\epsilon_{66}(\mathbf{i}) = \frac{1}{4\sqrt{2}} \sum_{\nu=1}^{4} (|\delta_{\mathbf{i},\nu}^{y}| - |\delta_{\mathbf{i},\nu}^{x}|), \tag{3}$$

where $\delta_{\mathbf{i},\nu} = (\delta_{\mathbf{i},\nu}^{x}, \delta_{\mathbf{i},\nu}^{y})$ $(\nu = 1, ..., 4)$ is the distance between Fe at $\mathbf{i}$ and one of its four neighbors As or Te (Fig. S1, Supplemental Material, Ref. [36]). The As/Te atoms move locally from their equilibrium position only along the x and y directions for simplicity. Both $\Psi_{\mathbf{i}}^{\mathrm{NN}}$ and $\epsilon_{66}(\mathbf{i})$ transform as the B_{1g} representation of the D_{4h} group.

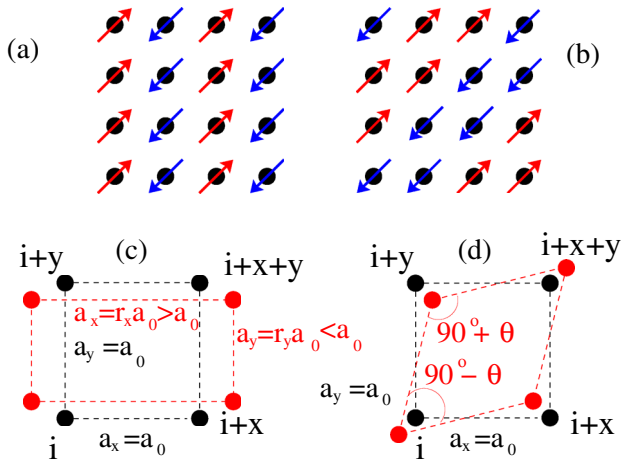

FIG. 1. (a) The collinear $(\pi, 0)$ AFM ordered state. (b) The bicollinear $(\pi/2, -\pi/2)$ AFM ordered state. (c) Schematic drawing of the Fe lattice equilibrium position in the $\mathcal{T}_{\mathrm{etra}}$ (black symbols) and $\mathcal{O}_{\mathrm{rth}}$ (red symbols) phases (four Fe's are indicated with filled circles and labeled by their site index $\mathbf{i}$). (d) Same as (c) but for the $\mathcal{M}_{\mathrm{ono}}$ case.

The crucial novel term $H_{\mathrm{SLM}} = -g_{12} \sum_{\mathbf{i}} \Psi_{\mathbf{i}}^{\mathrm{NNN}} \epsilon_{12}(\mathbf{i})$ introduced here provides the coupling between the spin and the $\mathcal{M}_{\mathrm{ono}}$ lattice distortion [42], with strength g_{12}. The spin NNN nematic order parameter is

$$\Psi_{\mathbf{i}}^{\mathrm{NNN}} = \frac{1}{2} \mathbf{S_i} \cdot (\mathbf{S_{i+x+y}} + \mathbf{S_{i-x-y}} - \mathbf{S_{i+x-y}} - \mathbf{S_{i-x+y}}). \tag{4}$$

$\Psi_{\mathbf{i}}^{\mathrm{NNN}}$ becomes 2 in the perfect $(\pi/2, -\pi/2)$ state of Fig. 1(b) [43]. $\epsilon_{12}(\mathbf{i})$ is the lattice $\mathcal{M}_{\mathrm{ono}}$ strain defined in terms of the Fe-Te/As distances $\delta_{\mathbf{i},\nu}$ as

$$\epsilon_{12}(\mathbf{i}) = \frac{1}{8} (|\delta_{\mathbf{i},2}| + |\delta_{\mathbf{i},4}| - |\delta_{\mathbf{i},1}| - |\delta_{\mathbf{i},3}|). \tag{5}$$

$\epsilon_{12}(\mathbf{i})$ transforms as the B_{2g} representation. For this reason, we must use $\Psi_{\mathbf{i}}^{\mathrm{NNN}}$, which also transforms as B_{2g}, in H_{SLM} so that it is invariant under the D_{4h} group. This simple symmetry argument is the reason why the bicollinear state is stabilized by the monoclinic distortion.

H_{SF} was studied with the same Monte Carlo (MC) procedure employed in Ref. [27] (see also Refs. [36,44]). Here, only a detailed description of the new lattice coupling $\tilde{g}_{12}$ will be provided. During the simulation, the As/Te atoms can move locally away from their equilibrium positions on the x-y plane, while the Fe atoms can move globally in two ways: (i) via an $\mathcal{O}_{\mathrm{rth}}$ distortion characterized by a global displacement (r_x, r_y) from the equilibrium position $(x_i^{(0)}, y_i^{(0)})$ of each iron with $r_\alpha = 1 + \Delta_\alpha$ $(\Delta_\alpha \ll 1;\ \alpha = x \text{ or } y)$ [Fig. 1(c)] and (ii) via a $\mathcal{M}_{\mathrm{ono}}$ distortion where the angle between two orthogonal Fe-Fe bonds is allowed to change globally to $90° + \theta$ with the four angles in the $\mathcal{M}_{\mathrm{ono}}$ plaquette adding to 360° so that the

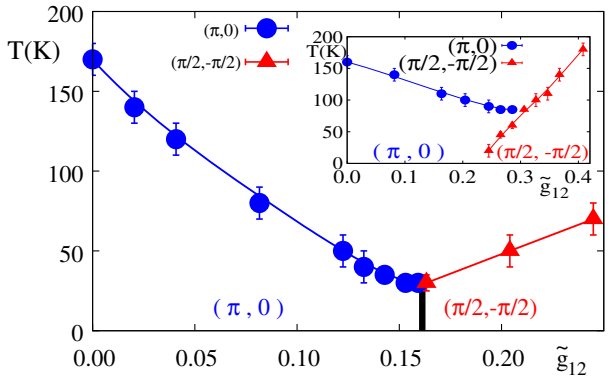

FIG. 2. Phase diagram along the straight line from $(\tilde{g}_{12}, \tilde{g}_{66}) = (0, 0.24)$ to (0.24,0), at $J_H = 0.1$ eV and $J_{\rm NN} = J_{\rm NNN} = 0$. Inset: Same phase diagram but along the straight line from $(\tilde{g}_{12}, \tilde{g}_{66}) = (0, 0.16)$ to (0.40,0), at $J_H = 0.1$ eV, $J_{\rm NN} = 0.012$ eV, and $J_{\rm NNN} = 0.008$ eV. Blue circles (red triangles) denote T_O (T_M), the transition temperatures to the $\mathcal{O}_{\rm rth}$/collinear ($\mathcal{M}_{\rm ono}$/bicollinear) phase.

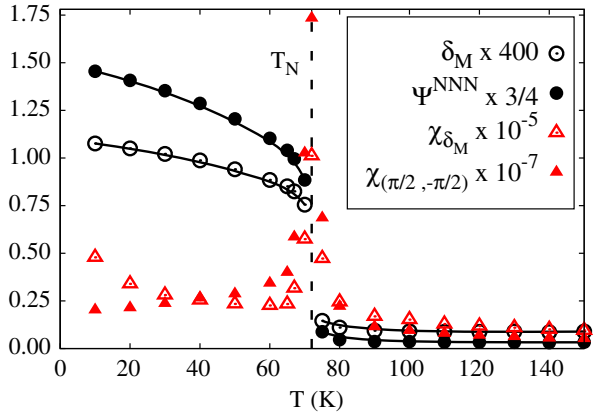

FIG. 3. Filled (open) circles indicate the bicollinear AFM order parameter $\Psi^{\rm NNN}$ (the $\mathcal{M}_{\rm ono}$ lattice distortion δ_M) at $\tilde{g}_{12} = 0.24$, $\tilde{g}_{66} = 0$, $J_H = 0.1$ eV, and $J_{\rm NN} = J_{\rm NNN} = 0$. Magnetic and lattice susceptibilities $\chi_{(\pi/2,-\pi/2)}$ and χ_{δ_M} are also shown (filled and open triangles, respectively). T_N denotes the first-order Neél temperature.

next angle in the plaquette becomes $90° - \theta$, with θ a small angle [Fig. 1(d)]. In addition, the localized (assumed classical) spins $\mathbf{S_i}$ and atomic displacements $(\delta^x_{\mathbf{i},\nu}, \delta^y_{\mathbf{i},\nu})$ that determine the $\mathcal{O}_{\rm rth}$ or $\mathcal{M}_{\rm ono}$ lattice distortion $\epsilon_{66}(\mathbf{i})$ [27,28] and $\epsilon_{12}(\mathbf{i})$ are also MC evaluated. In Ref. [36], the spin and lattice susceptibilities $\chi_{S(k_x,k_y)}$, χ_{δ_O}, and χ_{δ_M} and the dimensionless couplings $\tilde{g}_{66}$ and $\tilde{g}_{12}$ are defined.

Results.—In real chalcogenides, both B_{1g} and B_{2g} magnetic fluctuations should be present and the magnitude of their respective couplings to $\mathcal{O}_{\rm rth}$ and $\mathcal{M}_{\rm ono}$ distortions depends on doping, replacing Te by Se or iron excess, as in $Fe_{1+y}Te$. In addition, weak B_{2g} fluctuations may also exist in pnictides. For this reason, our study will address the MC phase diagrams, varying temperatures and couplings in a wide range. Consider first the case $J_{\rm NN} = J_{\rm NNN} = 0$. One of our most important results is in Fig. 2. At the left, a realistic $T_{\rm O}^{\rm max} \approx 170$ K is obtained for the transition to the collinear/$\mathcal{O}_{\rm rth}$ state, with an $\mathcal{O}_{\rm rth}$ distortion $\delta_O \approx 0.004$–0.008, compatible with experiments [9] and previous studies [27]. As $\tilde{g}_{12}$ increases and $\tilde{g}_{66}$ linearly decreases, then $T_{\rm O}^{\rm max}$ naturally decreases. When $\tilde{g}_{12} \approx 0.16$ and $\tilde{g}_{66} \approx 0.08$, remarkably now the FeTe bicollinear/$\mathcal{M}_{\rm ono}$ phase appears at T_M (red triangles). At the right in Fig. 2, the critical temperature is ~70 K similar to FeTe experiments [45]. Moreover, in the range shown, the monoclinic lattice distortions are small (for explicit values, see Fig. S4 of Ref. [36]) [46].

Bicollinear order is stabilized because with increasing $\tilde{g}_{12}$, the nematic order parameter $\Psi^{\rm NNN}_{\mathbf{i}}$ in $H_{\rm SLM}$ becomes nonzero to lower the energy. In each odd-even site sublattice, $\Psi^{\rm NNN}_{\mathbf{i}}$ favors a state with parallel spins along one diagonal direction and antiparallel in the other (equivalent to the collinear order but rotated by 45°). The parallel locking of the two independent spin sublattices leads to the state in Fig. 1(b) (or rotated ones).

As already explained, the purely fermionic SF model develops a collinear $(\pi, 0)$ tendency because of FS nesting in the tight-binding sector [26]. Since spin and lattice are linearly coupled, an $\mathcal{O}_{\rm rth}$ distortion is induced even for an infinitesimal $\tilde{g}_{66}$. On the other hand, regardless of $\tilde{g}_{66}$, the coupling $\tilde{g}_{12}$ needed to stabilize the bicollinear/$\mathcal{M}_{\rm ono}$ state is *finite* because it must first "fight" against the $(\pi, 0)$ order. However, in practice, this critical coupling is small ~0.1–0.25 and within experimental range.

To analyze the universality of the Fig. 2 phase diagram, we also investigated the effect of adding NN and NNN Heisenberg couplings along the line from $(\tilde{g}_{12}, \tilde{g}_{66}) = (0, 0.16)$ to (0.40,0) (inset of Fig. 2). Qualitatively, the results are similar. At (0.40,0) in the inset, the largest value of $\tilde{g}_{12}$ considered here, the $\mathcal{M}_{\rm ono}$ distortion is $\delta_M \approx 0.004$, still compatible with experiments [9]. One interesting difference, though, between the two cases is the appearance of an intermediate region at $\tilde{g}_{12} \approx 0.28$ in Fig. 2 (inset), where upon heating, a transition $\mathcal{M}_{\rm ono}$ to $\mathcal{O}_{\rm rth}$ is reached before the system eventually becomes paramagnetic. Experimentally, in $Fe_{1+y}Te$, an intermediate $\mathcal{O}_{\rm rth}$ phase with incommensurate magnetic order indeed exists between the $\mathcal{T}_{\rm etra}$ and $\mathcal{M}_{\rm ono}$ phases [45,47] with $T_O \approx 60$ K and $T_M \approx 50$ K, at $y \approx 0.13$. Our finite lattices do not have enough resolution to study the subtle incommensurate magnetism, but we conjecture that adding Fe to FeTe may effectively increase the spin-lattice coupling to reach the inset intermediate regime.

Another interesting result found here is that the bicollinear/$\mathcal{M}_{\rm ono}$ phase transition is strongly first order, as in experiments [9], as indicated by the order parameters discontinuities in Fig. 3 and by the MC time evolution histogram [Fig. 4(a)]. At high temperature, $(\pi, 0)$ fluctuations first develop (as implied by the inset of Fig. 2), leading to a free energy local minimum. However, upon

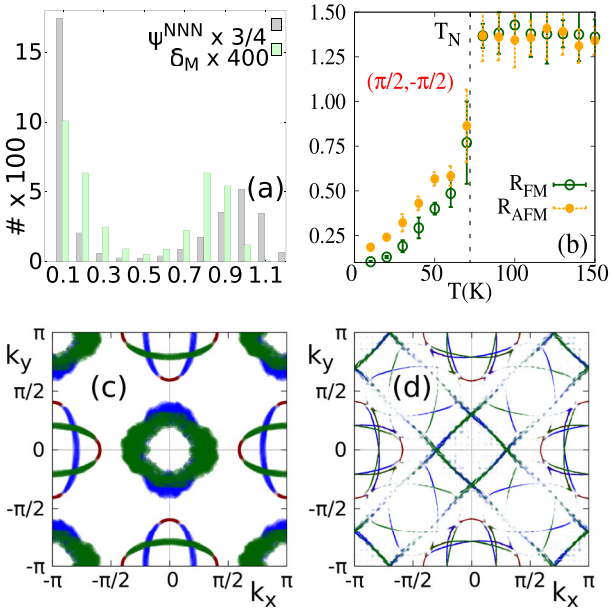

FIG. 4. (a) Histogram of the MC time evolution of Ψ^{NNN} and δ_M, at the critical temperature of Fig. 3 ($T = 72$ K), illustrating its bimodal character compatible with first-order characteristics. (b) Resistance ($h/2e^2$ units) vs temperature in the bicollinear state ($\tilde{g}_{12} = 0.24$, $\tilde{g}_{66} = 0$, $J_H = 0.2$ eV, no Heisenberg terms). Filled (open) symbols denote resistivities along the AFM (FM) direction. (c),(d) Symmetrized Fermi surface ($\tilde{g}_{12} = 0.24$, $\tilde{g}_{66} = 0$, $J_H = 0.2$ eV, no Heisenberg terms). (c) The high-temperature paramagnetic phase ($T = 360$ K). (d) The bicollinear phase ($T = 10$ K). The FS orbital composition notation is blue (xz), green (yz), and red (xy). In the nonsymmetrized FS (not shown), a gap opens along the AFM diagonal direction in the xz and yz orbitals, compatible with the resistivity results.

further cooling, the bicollinear minimum with a different symmetry also develops, and eventually a crossing occurs with first-order characteristics because one local state cannot evolve smoothly into the other.

Remarkably, the correct behavior for the resistivity anisotropy of FeTe [20,21] is also observed here (details are given in Ref. [36]). In the $(\pi, 0)$ phase, FS nesting opens a pseudogap for the yz orbital [26,27,48]. Because this orbital relates to electronic hopping along the ferromagnetic y axis, then the FM resistivity is the largest in pnictides. However, the *reversed* anisotropy with lower resistance along the FM direction (open circles) was found in the bicollinear phase [Fig. 4(b)] (the technique used is explained in Ref. [36]). Moreover, this reversed effect is amplified as J_H increases. The key clues to explain the effect are now clear: (i) an electron hopping along the plaquette diagonal in the AFM direction pays an energy J_H, but the hopping along the plaquette diagonal FM direction does not, and (ii) because FS nesting does not involve wave vectors such as $(\pi/2, -\pi/2)$, then pseudogaps are not created due to nesting, as in pnictides. Then, in essence, the reversed resistance found here is characteristic of large Hund coupling materials [49], such as manganites [10], where it is also known that the AFM direction is more resistive than the FM direction.

A paradox of FeTe is that first principles studies predict FS nesting and thus $(\pi, 0)$ order, as in pnictides. For this reason, we calculated the FS at couplings where the ground state is $\mathcal{M}_{\mathrm{ono}}$. Figure 4(c) shows the FS in the high-temperature $\mathcal{T}_{\mathrm{etra}}$ state. It is similar to that of the iron pnictides, suggesting $(\pi, 0)$ order upon cooling (the Γ centered features are blurry because of how a shallow pocket is affected by temperature). However, because of the sharp first-order transition, the $\mathcal{M}_{\mathrm{ono}}$ state reached at low temperature has a peculiar FS [Fig. 4(d)]: while the electron pockets are similar, the squarish Γ hole pocket is different from that of pnictides. In addition, "shadow bands" at $(\pm\pi/2, \pm\pi/2)$ develop, as in ARPES [7], indicative of couplings stronger than for pnictides [50].

Discussion.—Using computational techniques applied to the SF model, including a spin-lattice $\mathcal{M}_{\mathrm{ono}}$ distortion in the B_{2g} channel, we showed that the puzzling phenomenology of FeTe is well reproduced. This includes the presence of bicollinear magnetic order, $\mathcal{M}_{\mathrm{ono}}$ lattice distortions, a strong first-order $\mathcal{T}_{\mathrm{etra}}$-$\mathcal{M}_{\mathrm{ono}}$ transition, nested Fermi surfaces at high temperature naively favoring collinear order, and last but not least also the low-temperature reversed anisotropic resistances between the AFM and FM directions. Moreover, all this is achieved with spin-lattice dimensionless couplings less than 1 and with associated small lattice distortions $\delta_M \sim 10^{-3}$. While in pnictides the resistance anisotropy is related to FS nesting and a yz orbital pseudogap [48], in chalcogenides the strength of the Hund coupling is crucial. To our knowledge, the spin-lattice interaction discussed here provides the first comprehensive explanation of the challenging experimental properties of FeTe.

Discussions with S. Liang, P. Dai, and J. Tranquada are acknowledged. C. B. B. was supported by the National Science Foundation, under Grant No. DMR-1404375. E. D. and A. M. were supported by the U.S. Department of Energy, Office of Basic Energy Sciences, Materials Sciences and Engineering Division.

[1] D. C. Johnston, Adv. Phys. **59**, 803 (2010).
[2] P. C. Dai, J. P. Hu, and E. Dagotto, Nat. Phys. **8**, 709 (2012).
[3] Z. P. Yin, K. Haule, and G. Kotliar, Nat. Mater. **10**, 932 (2011).
[4] Recent results also indicate charge ordering in FeTe; see Wei Li, Wei-Guo Yin, Lili Wang, Ke He, Xucun Ma, Qi-Kun Xue, and Xi Chen, Phys. Rev. B **93**, 041101(R) (2016).
[5] Y. Zhang *et al.*, Phys. Rev. B **82**, 165113 (2010).
[6] Y. M. Dai, A. Akrap, J. Schneeloch, R. D. Zhong, T. S. Liu, G. D. Gu, Q. Li, and C. C. Homes, Phys. Rev. B **90**, 121114(R) (2014).

[7] Y. Xia, D. Qian, L. Wray, D. Hsieh, G. F. Chen, J. L. Luo, N. L. Wang, and M. Z. Hasan, Phys. Rev. Lett. **103**, 037002 (2009).

[8] The importance of the Hund coupling was also remarked within ARPES by P.-H. Lin, Y. Texier, A. Taleb-Ibrahimi, P. Le Fevre, F. Bertran, E. Giannini, M. Grioni, and V. Brouet, Phys. Rev. Lett. **111**, 217002 (2013).

[9] W. Bao *et al.*, Phys. Rev. Lett. **102**, 247001 (2009); S. Li *et al.*, Phys. Rev. B **79**, 054503 (2009).

[10] E. Dagotto, T. Hotta, and A. Moreo, Phys. Rep. **344**, 1 (2001).

[11] F. Ma, W. Ji, J. Hu, Z.-Y. Lu, and T. Xiang, Phys. Rev. Lett. **102**, 177003 (2009).

[12] C. Fang, B. A. Bernevig, and J. Hu, Europhys. Lett. **86**, 67005 (2009).

[13] In addition, discrepancies with neutron scattering have been unveiled; see O. J. Lipscombe, G. F. Chen, C. Fang, T. G. Perring, D. L. Abernathy, A. D. Christianson, T. Egami, N. Wang, J. Hu, and P. Dai, Phys. Rev. Lett. **106**, 057004 (2011); S. Chi, J. A. Rodriguez-Rivera, J. W. Lynn, C. Zhang, D. Phelan, D. K. Singh, R. Paul, and P. Dai, Phys. Rev. B **84**, 214407 (2011).

[14] Hartree-Fock real-space studies of the five-orbital Hubbard model without lattice distortions revealed a rich phase diagram [see Q. Luo and E. Dagotto, Phys. Rev. B **89**, 045115 (2014)]. Among the plethora of different magnetic states, the E phase was found, but in a very small and unrealistic region at large U and $n \sim 5.75$.

[15] The lattice degrees of freedom introduced here can be integrated out and generate a biquadratic term that favors bicollinear order; see S. Ducatman, R. M. Fernandes, and N. Perkins, Phys. Rev. B **90**, 165123 (2014).

[16] G. F. Chen, Z. G. Chen, J. Dong, W. Z. Hu, G. Li, X. D. Zhang, P. Zheng, J. L. Luo, and N. L. Wang, Phys. Rev. B **79**, 140509(R) (2009).

[17] D. Fobes *et al.*, Phys. Rev. Lett. **112**, 187202 (2014).

[18] Q. Huang, Y. Qiu, Wei Bao, M. A. Green, J. W. Lynn, Y. C. Gasparovic, T. Wu, G. Wu, and X. H. Chen, Phys. Rev. Lett. **101**, 257003 (2008).

[19] In Ref. [17], an electronic delocalization transition was proposed to lift the xz/yz orbital degeneracy, leading to ferro-orbital order along the ferromagnetic zigzag chains of the bicollinear state of $Fe_{1+y}Te$. See also I. Zaliznyak, A. T. Savici, M. Lumsden, A. Tsvelik, R. Hu, and C. Petrovic, Proc. Natl. Acad. Sci. U.S.A. **112**, 10316 (2015).

[20] L. Liu, T. Mikami, M. Takahashi, S. Ishida, T. Kakeshita, K. Okazaki, A. Fujimori, and S. Uchida, Phys. Rev. B **91**, 134502 (2015).

[21] J. Jiang, C. He, Y. Zhang, M. Xu, Q. Q. Ge, Z. R. Ye, F. Chen, B. P. Xie, and D. L. Feng, Phys. Rev. B **88**, 115130 (2013).

[22] See, e.g., discussion and citations in Ref. [1].

[23] I. A. Zaliznyak, Z. Xu, J. M. Tranquada, G. Gu, A. M. Tsvelik, and M. B. Stone, Phys. Rev. Lett. **107**, 216403 (2011).

[24] Other ARPES results were interpreted via polarons, as in manganites, also concluding that the lattice plays an important role; see Z. K. Liu *et al.*, Phys. Rev. Lett. **110**, 037003 (2013); Mechanisms relying on Jahn-Teller distortions, double exchange processes, and its associated Hund coupling, as in manganites, have also been discussed [see A. M. Turner, F. Wang, and A. Vishwanath, Phys. Rev. B **80**, 224504 (2009); M. Hirayama, T. Misawa, T. Miyake, and M. Imada, J. Phys. Soc. Jpn. **84**, 093703 (2015)].

[25] W.-G. Yin, C.-C. Lee, and W. Ku, Phys. Rev. Lett. **105**, 107004 (2010).

[26] S. Liang, G. Alvarez, C. Sen, A. Moreo, and E. Dagotto, Phys. Rev. Lett. **109**, 047001 (2012).

[27] S. Liang, A. Moreo, and E. Dagotto, Phys. Rev. Lett. **111**, 047004 (2013).

[28] S. Liang, A. Mukherjee, N. D. Patel, C. B. Bishop, E. Dagotto, and A. Moreo, Phys. Rev. B **90**, 184507 (2014).

[29] M. Daghofer, A. Nicholson, A. Moreo, and E. Dagotto, Phys. Rev. B **81**, 014511 (2010).

[30] The localized spins' magnitude is set to $S_i = 1$. Its actual value can be absorbed into the Hamiltonian parameters.

[31] Any ratio larger than $1/2$ leads to similar results.

[32] A complete study of the bicollinear magnetic state requires a five-orbital Hubbard model, plus the lattice, all at finite temperatures. Such a formidable challenge is not practical: the SF model is a simplification that allows for the study of structural, orbital, and magnetic effects simultaneously.

[33] R. M. Fernandes, A. V. Chubukov, J. Knolle, I. Eremin, and J. Schmalian, Phys. Rev. B **85**, 024534 (2012).

[34] R. M. Fernandes and J. Schmalian, Supercond. Sci. Technol. **25**, 084005 (2012).

[35] The spin in H_{SLO} and H_{SLM} is only the localized spin for computational simplicity.

[36] See Supplemental Material at http://link.aps.org/supplemental/10.1103/PhysRevLett.117.117201, which includes Refs. [37–41], for technical details of the lattice degrees of freedom and their Monte Carlo update, numerical values for the lattice distortions and spin structure factors varying couplings, and resistivity plots also at various sets of parameters.

[37] Q. Huang, Y. Qiu, Wei Bao, M. A. Green, J. W. Lynn, Y. C. Gasparovic, T. Wu, G. Wu, and X. H. Chen, Phys. Rev. Lett. **101**, 257003 (2008).

[38] J. Salafranca, G. Alvarez, and E. Dagotto, Phys. Rev. B **80**, 155133 (2009).

[39] J. A. Vergés, Comput. Phys. Commun. **118**, 71 (1999).

[40] M. A. Tanatar *et al.*, arXiv:1511.04757 [Phys. Rev. Lett (to be published)].

[41] J-H. Chu, J. G. Analytis, K. De Greve, P. L. McMahon, Z. Islam, Y. Yamamoto, and I. R. Fisher, Science **329**, 824 (2010).

[42] H.-H. Kuo, J.-H. Chu, S. A. Kivelson, and I. R. Fisher, Science **352**, 958 (2016).

[43] The degeneracy of the bicollinear states with momentum $(\pi/2, \pi/2)$ and $(\pi/2, -\pi/2)$ is broken by the $\mathcal{M}_{\mathrm{ono}}$ distortion. Here, we assume that the state with momentum $(\pi/2, -\pi/2)$ is stabilized.

[44] The physical range for J_H, J_{NN}, and J_{NNN} was also extensively discussed before in Refs. [26,27] (see Ref. [36] as well).

[45] Y. Mizuguchi, K. Hamada, K. Goto, H. Takatsu, H. Kadowaki, and O. Miura, Solid State Commun. **152**, 1047 (2012).

[46] The low-temperature (10 K) phase diagrams varying $\tilde{g}_{66}$ and $\tilde{g}_{12}$ are also in Ref. [36] [see Fig. S2 (S3) with (without)

Heisenberg couplings]: in a broad range of couplings, the bicollinear/$\mathcal{M}_{\text{ono}}$ state is spontaneously stabilized.

[47] E. E. Rodriguez, C. Stock, P. Zajdel, K. L. Krycka, C. F. Majkrzak, P. Zavalij, and M. A. Green, Phys. Rev. B **84**, 064403 (2011).

[48] M. Daghofer, Q.-L. Luo, R. Yu, D. X. Yao, A. Moreo, and E. Dagotto, Phys. Rev. B **81**, 180514(R) (2010).

[49] Chalcogenides have higher magnetic moments than pnictides and thus likely larger Hund couplings. We also noticed that for $J_H = 0.1$ eV, we found that the reversed anisotropy was still there but reduced (see Supplemental Material, Ref. [36]).

[50] Nesting tendencies, even if not crucial, could potentially lead to phase separation effects [A. O. Sboychakov, A. V. Rozhkov, K. I. Kugel, A. L. Rakhmanov, and F. Nori, Phys. Rev. B **88**, 195142 (2013)]. While we checked that phase separation is not present in our model, in the undoped regime studied, it may occur upon doping.